Development of Cu nanoflowers modified the flexible needle-type microelectrode and its application in continuous monitoring glucose in vivo

Yuxin Fang, Shenjun Wang, Yangyang Liu, Zhifang Xu, Kuo Zhang, Yi Guo

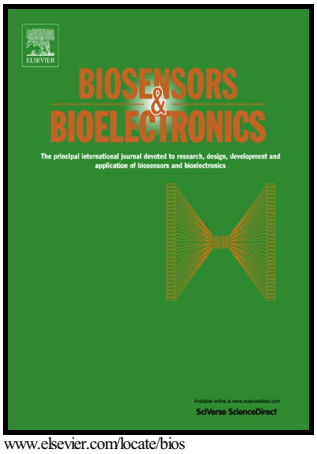

www.elsevier.com/locate/bios

PII: S0956-5663(18)30198-2
DOI: https://doi.org/10.1016/j.bios.2018.03.024
Reference: BIOS10350

To appear in: *Biosensors and Bioelectronic*

Received date: 29 December 2017
Revised date: 9 March 2018
Accepted date: 12 March 2018

Cite this article as: Yuxin Fang, Shenjun Wang, Yangyang Liu, Zhifang Xu, Kuo Zhang and Yi Guo, Development of Cu nanoflowers modified the flexible needle-type microelectrode and its application in continuous monitoring glucose in vivo, *Biosensors and Bioelectronic,* https://doi.org/10.1016/j.bios.2018.03.024

Development of Cu nanoflowers modified the flexible needle-type microelectrode and its application in continuous monitoring glucose in vivo

Yuxin Fang*, Shenjun Wang, Yangyang Liu, Zhifang Xu, Kuo Zhang, Yi Guo*

Research Center of Experimental Acupuncture Science, College of Acumox and Tuina, Tianjin University of Traditional Chinese Medicine, Tianjin 300193, PR China

meng99_2006@126.com

guoyi_168@163.com

*Corresponding author. Tel./fax: +86 22 59596211.

*Corresponding author. Tel./fax: +86 22 59596211.

Abstract

A minimally invasive glucose microbiosensor based the flexibly integrated electrode for continuous monitoring glucose in vivo has been developed in this study. This was achieved by coating needle-type microelectrode with Cu nanoflowers, nafion, glucose oxidase (GOD) and polyurethane (PU) membranes, successfully prepared with layer-by-layer deposition. The Cu nanomaterials provided a large specific surface area and electrocatalytic activity for glucose detection. The PU layers as mass-transport limiting membranes significantly enhanced the linearity and stability of sensors. The resulting biosensor exhibited a wide linear range of 0 to 20 mM, with a good sensitivity of 42.38 nA mM^{-1} (correlation coefficient r^2 was 0.99)

and a fast response time of less than 15s. In vivo implantable experiments using anesthetized rats showed excellent real-time response to the variation of blood glucose concentration. And the variation tendency of sensor output was consistent with that using the glucose meter. Overall, the results supported the suitability of this microsensor for measuring rapid changes of glucose in vivo. This work offers a promising approach in implantable device applications related to diabetes management as well as other medical diagnosis.

Keywords: glucose sensor; in vivo; Cu nanoflowers; polyurethane; microelectrode

1. Introduction

Diabetes mellitus is one of the factors of death that can affect individuals be unable to maintain normal glucose levels. 382 million people suffered from diabetes in 2013(Guariguata et al., 2014), and it's anticipated that 20% and 69% of all the people in developed and developing countries may be diagnosed as the diabetics by 2030(Cleland et al., 2016). So far, continuous blood glucose motitoring devices are widely used in diabetes mellitus to provide variation information about blood glucose levels throughout the day(Battelino et al., 2012; Renard and Eric, 2002). However, the conventional self-glucose monitoring methods have some limitations in accuracy for analyzing the status or detection of low glucose level(Lee et al., 2016; Lee et al., 2013). Therefore, it is of great significance to develop continuous glucose monitoring device for promoting the present situation (Schmelzeisen-Redeker et al., 2013). For the moment, the glucose biosensors are widely used in this field(Gu et al., 2014; Lourenço

et al., 2016; Yu et al., 2013).

Glucose oxidase (GOD)-based glucose detection offers less severe conditions during the preparation procedure and storage owing to its specificity to glucose, the high activity over a wide range of pH, and thus has been widely used in glucose monitoring(Wang et al., 2013; Wilson and Turner, 1992). However, the direct contact of GOD with bare electrode surface often changes the structure and function of GOD and loses biological activity(Huang et al., 2013). So some efforts have been made to improve electron transfer of GOD on the electrode surface(Buk et al., 2017; Caldas et al., 2017; Guo et al., 2017). One promising method is to employ nanomaterials which have a high surface area, good biocompatibility and catalytic properties.

Metal nanomaterials have received tremendous scientific and practical interest owing to their unique properties and novel applications compared to their bulk counterparts(Fang et al., 2015; Huang et al., 2009; Huang et al., 2013; Lin et al., 2016; Lu et al., 2016; Wang et al., 2017). As one of the most conventional metals, copper (Cu) and Cu oxides-based nanomaterials have been widely investigated due to their low cost, high electrical conductivity and being free from chloride poisoning(Wang et al., 2012; Zhang et al., 2012). In addition, it has been well-established that the shape, size and the morphology of the metal nanostructures can effectively tune their properties by exposing different lattice planes and providing different numbers of active sites(Lu and Chen, 2012; Qin et al., 2012). So in the development and investigation of metal nanoparticles, it is very important to synthesize them through controlling different experimental conditions. Among various specific nanostructures, three–dimensional

nanoflowers materials have received increasing interest due to the unique physical and chemical properties.

In this paper, a kind of flexibly integrated microelectrode which contained working electrode and reference/counter electrode was prepared at first. Taking advantage of the Cu nanoflowers, the novel nanomaterials were designed for glucose biosensor construction. The Cu nanoflowers were prepared by one-step electrodeposition technique under the control of the certain Cu^{2+} concentration and electrodeposition time. Flower shaped Cu nanostructures offered lower redox potential operating system(Annamalai et al., 2012), high specific surface area and more active sites to promote electro-catalysis of glucose on electrode. The nafion layer was used here to improve anti-interference performance of sensor and provide micro-bioenviroment for glucose oxidase. The immobilization of glucose oxidase on Pt microelectrode was carried out by covalent attachment with glutaraldehyde and bovine serum albumin (BSA). In addition, in order to enlarge linear response range as well as improve the stability and biocompatibility of implanted glucose sensors, polyurethane (PU) was employed here as an outer membrane to act as a limiting diffusion layer and biocompatible interface with the surrounding host tissue. The role of the limiting diffusion layer is extremely important to sensor function. It can serve as a barrier membrane to reduce the enzyme leaching and also serve to limit the diffusion of glucose relative to oxygen, maximizing the sensor's dynamic response to glucose(Shin et al., 2004). The in vitro electrochemical performances of the as-prepared microsensor were investigated by cyclic volatmmetry and

chronoamperometry. The microsensor exhibited good sensitivity and large linear response range. In vivo implantable experiments using anesthetized rats showed excellent real-time response to the variation of blood glucose concentration.

2. Experimental

2.1. Reagents

Glucose oxidase from Aspergillus niger(GOD, EC 1.1.3.4, p*I* 4.2, 235 Units mg^{-1} protein), nafion, bovine serum albumin (BSA), ascorbic acid (AA), uric acid (UA) and acetaminophen (DA) were purchased from Sigma Co. Tecoflex SG-85A polyurethane (PU) was purchased from Lubrizol Co.. Glutaraldehyde (25%), tetrahvdrofuran (THF), dimethylformamide (DMF), $CuSO_4$, K_2SO_4 and glucose were reagent grade and purchased from Tianjin damao Chemical Reagent Co. (China). 3mg mL^{-1} of GOD and 10 mg mL^{-1} BSA were prepared in 0.1M phosphate buffer solution (PBS, pH 7.4). All aqueous solutions were prepared with doubly distilled water.

2.2. Apparatus

All electrochemical measurements were performed using a CHI 660 electrochemical workstation (Beijing CHI Instruments). Blood glucose concentration from rat's tail tip was measured by a glucose meter (ACCU-CHEK Active, Switzerland). The surface morphology studies were carried out using field emission scanning electron microscope (FESEM), Nova NanoSEM 430 (FEI, USA). Electrode appearance scanning microscopy was handled using 3D laser scanning confocal microscope (OLS4000, OLYMPUS Co.). Transmission electron microscopy (TEM) images was obtained by using Tecnai G2 F20 instrument (Philips Holland) equipped

with an energy-dispersive X-ray spectroscopy (EDX) analyzer. The phase purity and crystalline nature of the prepared Cu nanoflowers product was studied using the powder X-ray diffraction technique (XRD, Rigaku, Cu Kα radiation operating at 40 KeV/40 mA). The elemental composition and its electronic states were obtained using X-ray photoelectron spectroscopy (XPS; Axis Ultra spectrometer) with an Al-Kα X-ray source.

2.3. Preparation and modification of glucose biosensor

The flexibly integrated needle-type electrode was prepared according to previously reported method (Aussedat et al., 2000; Bindra et al., 1991; Wilson et al., 1992)with some modifications. As shown in Fig.1(A-E), the diameter of Pt wire which acted as the working electrode is 0.2 mm, and the overall diameter at the widest point (containing reference/counter electrode) is approximately 0.4-0.5 mm. Pt wire was coated with insulating layer except for about 1-2 mm length which is reaction region exposed at the front of 2 mm from the tip. The coaxial reference/counter electrode was formed on the insulating layer surface. A thin silver wire (0.05 mm o.d.) was tightly wrapped around the insulating layer surface covering about 3 mm of its length. The back-end nonbinding silver wire and Pt wire were fixed by insulating tube and respectively provided with a terminal used for being connected with the electrode clamp. A layer of silver chloride was formed by passing current (0.4 mA/cm^2) for 2h through the wrapped silver wire while it was dipped in a stirred 0.1 M HCl solution. The reference/counter electrode was rinsed with deionized water for 6 h. For the prepared microelectrode was extremely flexible, it could be implanted into body by

using a disposable sterile syringe needle, which was removed after the electrode is in place.

Fig.1. The fabrication of needle-type microelectrode. (A) The structure diagram of microelectrode. (B-E) The 3D laser scanning confocal microscope images of microelectrode at different position.

The electrode modification process was as follows: the bare electrode was first degreased by washing with acetone and ethyl alcohol, and then it was rinsed with deionized water and dried with N_2. For Cu nanoflowers preparation, the electrode was carried out by a potential step to -1.0 V vs. Ag/AgCl for a period of 20 min in the stationary electrolyte solution composed of 0.3 mol L^{-1} $CuSO_4$ and 0.1mol L^{-1} K_2SO_4. After dip coating with nafion solution, the electrode was kept in drying oven of 120 ℃ for 1h. And when the electrode restored to room temperature, the glucose biosensor was constructed by mixing 125 μL GOD (3 mg mL^{-1}), 25μL BSA (10 mg mL^{-1}) and 20μL glutaraldehyde (2%) solution, and then 5 μL of the composite solution was dropped on the reaction region of the electrode. The electrode was stored at room temperature and GOD had been cross-linked for 2h. After that the electrode was optionally dip-coated in the 5% (w/w) PU in 98% (w/w) THF, 2% (w/w) DMF solution. This PU coating step could be repeated for 2-3 times if the desired linear range was not obtained after the first coating. The microelectrode was washed with deionized water and dried at room temperature.

2.4. In vitro evaluation and characterization

The in vitro evaluation of prepared glucose biosensors for measurement of glucose

was performed by amperometry at +0.6V. The experiments were carried out in 40 mL PBS (0.1 M, pH 7.4) at room temperature under gentle stirring after a 1h period of current stabilization. Analytical and kinetic parameters were determined after baseline stabilization by adding aliquots of the stock glucose solution to obtain final concentrations in the range of 0-40mM. The electrodes sensitivities were measured every few days in PBS with the glucose linear concentration in the range of 0-20mM. The selectivity against major interferents was determined by additions of glucose (4mM), ascorbic acid (0.1mM), uric acid (0.5mM), dopamine (0.1mM) and glucose (4mM) successively. In order to get the good sensitivity and linear detection range for glucose, optimization preparing process of the Cu nanomaterials was investigated. In addition, the apparent Michaeli-Menten constant (K_m) of modified GOD was also studied.

2.5. In vivo experiments

In vivo studies were carried out on adult male Wistar rats maintained in controlled environmental conditions. Rats were anesthetized with pentobarbital sodium and fixed on the operating plate. The prepared glucose biosensor electrodes were implanted under the skin of cervical dorsal using disposable sterile syringe needles, which were removed after the electrodes were in place. The front about 8 mm of the electrode was located under the skin and the remaining parts connecting leads were exposed to the outside for connection to the potentiostat during tests. At last, the electrodes were immobilized by medical plasters and prevent to be pulled out by the rats.

Amperometric recordings were started and the background currents were allowed

to stabilize for 2h. Once the background currents were stable, glucose was injected through tail vein during specific time intervals. The overall detection time was approximately 4h, and the anesthetic was replenished at any time through tail vein when the rats were about to wake up.

3. Results and discussion

3.1. Characterization of the modified microelectrodes

In this work, the Cu nanoflowers film was fabricated on the bare Pt microelectrode with electrodeposition method. The electrochemical properties can be affected by the morphology and structure of the materials. The surface morphology of the as-prepared Cu nanoflowers product was characterized by FESEM and TEM. Fig. 2 (A, B) showed the FESEM images of different magnification of the Cu nanoflowers, electrochemically deposited at -1.0 V in the solution of 0.3 mol L^{-1} $CuSO_4$+0.1mol L^{-1} K_2SO_4 for 20 min. A low magnification image of Cu is shown in Fig. 2A. It is obvious that the Cu nanostructures are of three-dimensional interconnected flower structures consisting of crystal each nanocluster with some petal-like form. From the high magnification image in Fig. 2B & inset of Fig. 2B, the nanoclusters are assembled by large amounts of stackable nanocubes. Fig. 2C also shows a typical TEM image of Cu nanoflowers. The results showed that Cu nanocubes were firstly formed, which is similar to the literature(Wang et al., 2017; Yang et al., 2010). When follow up reduced Cu was deposited on the surface of Cu nanocubes, the growth rate at the outer edge is much faster than at inner sites, resulting flower shaped structures which were more easily formed on the vertical angle of the cube. Additionally, the energy-dispersive

X-ray spectrum(EDX) analysis was performed to characterize the chemical composition of Cu nanoflowers (Fig.2D) and to confirm the presence of the pure elements: Cu. The C in the spectrum should be from the substrate. The powder X-ray diffraction patterns of the synthesized Cu nanoflowers is shown in Fig. 2E. Three peaks at $2\theta = 43.3°$, 50.4° and 73.6°, corresponding to Miller indices (111), (200) and (220), could be indexed to the face-centered cubic lattice of Cu (0) (JCPDS 04-0836), which is in good accordance with reported data(Huang et al., 2013; Zhang et al., 2013).

Fig. 2F presents the XPS spectra to analyse the surface electronic state of Cu. From the high resolution spectrum of the Cu 2p region, we can see two strong peaks at about 931.8 and 951.6 eV are associating with the binding energy of Cu $2p_{3/2}$ and Cu $2p_{1/2}$ electrons, respectively, which is in good agreement with pure copper (Radhakrishnan et al., 2016; Tian and Liu, 2013).

This Cu nanostructures deposited onto the Pt microelectrode could give rise to a large surface area and good electrochemical property towards glucose detection compared with the bare electrode. The electron-transfer mechanism on the modified electrode is shown in Fig.2G, H_2O_2 which is generated by glucose oxidation reaction can be adsorbed on the surface of Cu nanoflowers, and the O-O bond of H_2O_2 can be broken up into double OH· radical by Cu(0) in Cu nanoflowers (Gao et al., 2007; Jv et al., 2010). This may result in the catalytic ability of Cu nanostructures, consequently the electro-catalytic property of biosensors could be improved.

Fig. 2. FESEM images of the Cu nanoflowers with (A) low magnification and (B) high magnification. (C) TEM image of Cu nanoflowers product. (D) EDX spectrum of Cu nanoflowers. (E) X-ray diffraction pattern of Cu nanoflowers. (F) High-resolution X-ray photoelectron spectroscopy survey spectrum of Cu nanoflowers. (G) The principle of operation towards glucose.

3.2. Optimization of the Cu nanoflowers modified microelectrode

It was found that the morphology and size of Cu nanostructures were decided by the concentration of $CuSO_4$ and electrodeposition potential, sequentially the electrochemical performances of the whole sensing towards glucose were affected. Here for getting the good sensitivity and linear detection range for glucose, concentration of $CuSO_4$ and electrodeposition potential were investigated by changing single condition while others were fixed.

The influence of concentration of Cu^{2+} on Cu morphology was explored by SEM (Fig. S1). The results showed that Cu nanocubes were firstly formed in 10 mM $CuSO_4$ solution under -1V for 20 min (Fig. S1 A), then grew gradually and formed tree shape when the concentration of Cu^{2+} increased to 200 mM (Fig. S1 B-D). And the flower shape formed lastly when concentration of Cu^{2+} increased to 300 mM (Fig. S1 E). With further increase of Cu^{2+} concentration, no obvious shape changes were observed. The influence of electrodeposition potential on Cu morphology had similar effects.

From Fig. S2, the current response increased with increasing concentration of Cu^{2+} from 10mM to 500mM to reach the maximum and smooth thereafter. It was discovered when concentration of Cu^{2+} was 300mM, the uniform Cu flower

nanostructures was formed. And this Cu structures was fit for adsorption and catalyzation of H_2O_2 and thereby the most detection current of glucose was get. The electrodeposition potential is another variable that affects the current response of the modified electrodes. The effect of electrodeposition potential on current response of the sensor has been investigated and the corresponding result was shown in Fig. S3. The peak current for glucose detection increased with the increasing of the electrodeposition potential until -1V. It proved that this potential was the most suitable for the growth of homogeneous Cu nanoflowers. So the $CuSO_4$ solution concentration of 300mM and the electrodeposition potential of -1V were selected as the optimized conditions in this work.

3.3. Stability in vitro of the sensor

The stablity in vitro of the sensor was evaluated by storing the microelectrode in PBS at 37℃and testing the response current under a constant potential of 0.6V as well as sensitivity changes every few days. As shown in Fig 3(A, B), repeated testing of sensor function displayed that the response current and relative sensitivity typically increased up to 6 days (and a corresponding decrease in linearity) and then remained stable for the rest of the study period of 20 days. This result brings into correspondence with the reported studies(Bindra et al., 1991; Wang et al., 2013; Yu et al., 2005). The initial increase was attributed to the swelling of enzyme and PU membranes, resulting in the increase of membrane permeability. More glucose could pass through the protective membrane and the sensor sensitivity increased in the initial period of time, and the correspongding linear range was decrease in the

meanwhile. After 6 days, with the membrane structures tended to stable, the impact of PU mass-transport-limiting membrane layers played dominant role. Finally the sensor's sensitivity remained stable until 20 days. So the long-time glucose detection and stability of sensor could be guarantee.

Fig. 3. (A) Amperometric responses of biosensors every few days towards various concentration of glucose dropwise added into 0.1 M PBS solution under stirring. (B) Relative stability test of the prepared biosensors stored in PBS.

3.4. Electrocatalytic performance of the sensor towards glucose

The performance tests behind were all operated when the electrodes were stored for 6 days in PBS, which the sensitivity of this sensor became stable. Amperometric responses of microsensor to successive addition of 4 mM glucose in 0.1 M stirring PBS solution (pH 7.4) under the applied potential of 0.6 V vs. Ag/AgCl was given in Fig. 4A. As can be seen, when the glucose of certain concentration was added into the PBS solution, the oxidation current of modified electrode increased gradually. The 95% of the steady-state current was obtained within 15 s. The corresponding calibration curve was presented in Fig. 4B. The amperometric response current showed a linear variation with increasing concentration of glucose over the range from 0 to 20 mM. The sensitivity of the fabricated biosensor was calculated from the slope of the curve and found to be 42.38 nA mM^{-1} (correlation coefficient r^2 is 0.99).

Fig. 4. (A) Amperometric responses of the prepared biosensor towards various concentration of glucose dropwise added into 0.1 M PBS solution

under stirring, work potential: 0.6 V vs. Ag/AgCl. (B) Calibration curve of the amperometric responses vs.various glucose concentrations.

The comparison of different electrochemical sensors for the determination of glucose was given in Table 1. It can be seen that this new biosensor exhibits a wider linear range. It is suitable for detecting human blood glucose concentration for the diagnosis of diabetes mellitus, since the normal range of blood glucose concentration is 4.4-6.6 mM.

Table 1 The comparison of different electrochemical sensors for the determination of glucose.

The kinetic parameter, apparent Michaeli-Menten constant (K_m) can be calculated according to the Lineweaver–Burk equation:

$$\frac{1}{I_{ss}} = \frac{K_m}{I_{max}} \frac{1}{C} + \frac{1}{I_{max}}$$

As shown in Fig. S4, the maximum sensing current was 2.61μA and the apparent Michaeli-Menten constant (K_m) was 40.5 mM. This apparent K_m value was higher than that (33mM) of the soluble GOD from *A. niger*(Almeida et al., 1993). The higher K_m value of the immobilized GOD gave the evidence of a superposition of diffusional and kinetic limitation, which means the wider linearity of the sensor and indicates larger glucose detection range(Fang et al., 2017).

The general problem in the electrochemical detection of glucose is the interference from physiological species such as ascorbic acid (AA), uric acid (UA), and dopamine (DA), etc. The selectivity of the present glucose biosensor against these possible

interfering species was studied by comparing the amperometric responses of physiological levels of various electroactive species (0.1 mM AA, 0.5 mM UA and 0.1 mM DA) and glucose (4 mM) at the potential of 0.6 V vs. Ag/AgCl in Fig. 5. The prepared sensor did not give significant response to the interference species of AA, UA and DA while maintaining high sensitivity to glucose. This result exhibited that the modified layer of electrode could achieve reliable permselectivity.

Fig. 5. Interference test of prepared biosensor in 0.1 M PBS solution at the working potential of 0.6 V with 4 mM glucose (twice) and other interfering substance (0.1 mM AA, 0.5 mM UA and 0.1 mM DA).

3.5. In vivo experiments using implantable biosensors

In vivo experiments, rats were anesthetized with pentobarbital sodium and fixed on the operating plate. The prepared flexible microelectrodes were implanted under the skin of cervical dorsal using disposable sterile syringe needles, which was removed after the electrode is in place (Fig. 6A). The sensor leads were attached to a CHI 660 potentiostat with a 0.6 V Ag/AgCl potential. Current versus time data was continually recorded on the potentiostat. As shown in Fig. 6B, the response current of the sensor reached a stable value after a run-in period of 2 h. This stable time in vivo was much longer than that in vitro, which was because that the glucose diffusion in tissue fluid is much lower than in vitro(Dungel et al., 2008). Prior to in vivo monitoring of glucose, the normal saline (NS) was first injected into the rats body through caudal vein catheter, and the NS did not provoke any change in the baseline current except for some disturbance. And with injection of 0.4mL of glucose (4M) into the rats body

through caudal vein catheter, the current response was clearly visible. As can be seen from the Fig. 6B, the sensor response current started to rise after the glucose injection and reached the peak approximately 5min later, and then remained at the plateau value for a few seconds before falling toward the baseline. Through 2 times injection of 0.4mL of glucose (4M), the consistent amplitude response could be seen.

In Fig. 6C, the sensor readings were compared with blood glucose measurements made using a glucose meter. Discrete blood glucose measurements were performed in parallel from the tail tip prick using glucose testing strips. As shown in Fig. 6C, the sensor output variation tendency followed well with the blood glucose concentration change tested from tail tip using glucose meter throughout the entire experiment. However, there was a signal delay of about 3-5 min between the value reported by the implanted sensor and the blood glucose concentration tested from the tail tip. This was ascribable to the sensor itself, circulatory transport from the central venous infusion site to the implant site, as well as mass transfer and physiologic phenomena within the local tissues(Gough et al., 2010). This time delay value is consistent with other reported studies(Chen et al., 2015; Fang et al., 2017; Gough et al., 2010).

Fig. 6. In vivo continuous monitoring of glucose concentration in rat. (A) Image of glucose biosensor implantation into rat back. (B) Implanted sensor current response to twice glucose injection. (C) The in vivo response of the implanted sensor to glucose injection (black line) compared with blood glucose values measured from the tail tip tested by a glucose meter (blue line).

4. Conclusions

In this work we reported the development of a flexibly integrated microelectrode which was coated by Cu nanoflowers/nafion/GOD/PU structures suitable for transcutaneous implantation. The Cu nanostructures improved the response current of the sensor, which was due to its high catalytic activity, large accessible surface area and good conductivity. The nafion membrane provided excellent anti-interference property. And the PU layer supplied an optimal balance between oxygen and glucose transport to the sensing layer and improved the stability of the protective layer. The sensors showed a good reproducibility when measured in PBS. The in vivo implantable experiments supported their suitability for testing the variation of blood glucose. Besides, the sensor output variation tendency followed well with the blood glucose concentration change tested from tail tip using the glucose meter throughout the entire experiment. It confirmed that the prepared sensor was a mean of arriving at a fairly reliable glucose detecting in vivo. This work offers a promising approach in implantable device applications related to diabetes management as well as other medical diagnosis.

Acknowledgment

The financial supports from National Natural Science Foundation of China (Grant Nos. 81503636 and 81704146) and Application Basis and Advanced Technology Research Project of Tianjin (Grant No. 15JCQNJC10800) are acknowledged.

References:

Almeida, N.F., Beckman, E.J., Ataai, M.M., 1993. Biotechnol. Bioeng. 42(9), 1037-1045.

Amouzadeh Tabrizi, M., Varkani, J.N., 2014. Sensor. Actuat. B-Chem. 202, 475-482.

Annamalai, S.K., Palani, B., Chandrasekara Pillai, K., 2012. Colloid Surface A 395, 207-216.

Aussedat, B., Dupire-Angel, M., Gifford, R., Klein, J.C., Wilson, G.S., Reach, G., 2000. Am. J. Physiol-Endoc. M. 278(4), E716-E728.

Battelino, T., Conget, I., Olsen, B., Schütz-Fuhrmann, I., Hommel, E., Hoogma, R., Schierloh, U., Sulli, N., Bolinder, J., The, S.S.G., 2012. Diabetologia 55(12), 3155-3162.

Bindra, D.S., Zhang, Y., Wilson, G.S., Sternberg, R., Thevenot, D.R., Moatti, D., Reach, G., 1991. Anal. Chem. 63(17), 1692-1696.

Buk, V., Emregul, E., Emregul, K.C., 2017. Mat. Sci. Eng: C 74(Supplement C), 307-314.

Caldas, E.M., Novatzky, D., Deon, M., de Menezes, E.W., Hertz, P.F., Costa, T.M.H., Arenas, L.T., Benvenutti, E.V., 2017. Micropor. Mesopor. Mat. 247(Supplement C), 95-102.

Chen, D., Wang, C., Chen, W., Chen, Y., Zhang, J.X., 2015. Biosens. Bioelectron. 74, 1047-1052.

Cleland, C.R., Burton, M.J., Hall, C., Hall, A., Courtright, P., Makupa, W.U., Philippin, H., 2016. Lancet Diabetes Endo. 4(1), 10-12.

Dungel, P., Long, N., Yu, B., Moussy, Y., Moussy, F., 2008. J. Biomed. Mater. Res. A 85(3), 699-706.

Fang, L., Liang, B., Yang, G., Hu, Y., Zhu, Q., Ye, X., 2017. Biosens. Bioelectron. 97, 196-202.

Fang, L., Liu, B., Liu, L., Li, Y., Huang, K., Zhang, Q., 2016. Sensor. Actuat. B-Chem. 222, 1096-1102.

Fang, Y., Zhang, D., Guo, Y., Guo, Y., Chen, Q., 2015. Sensor. Actuat. B-Chem. 221(Supplement C), 265-272.

Gao, L., Zhuang, J., Nie, L., Zhang, J., Zhang, Y., Gu, N., Wang, T., Feng, J., Yang, D., Perrett, S., Yan, X., 2007. Nat. Nanotechnol. 2(9), 577-583.

Gough, D.A., Kumosa, L.S., Routh, T.L., Lin, J.T., Lucisano, J.Y., 2010. Sci. Transl. Med. 2(42), 42-53.

Gu, H., Yang, Y., Zhou, X., Zhou, T., Shi, G., 2014. J. Electroanal. Chem. 730(Supplement C), 41-47.

Guariguata, L., Whiting, D.R., Hambleton, I., Beagley, J., Linnenkamp, U., Shaw, J.E., 2014. Diabetes Res. Clin. Pr. 103(2), 137-149.

Guo, Q., Liu, L., Zhang, M., Hou, H., Song, Y., Wang, H., Zhong, B., Wang, L., 2017. Biosens. Bioelectron. 92(Supplement C), 654-660.

Huang, H., Wu, Y.Q., Wang, S.L., He, Y.H., Zou, J., Huang, B.Y., Liu, C.T., 2009. Mat. Sci. Eng. A-Struct. 523(1), 193-198.

Huang, J., Dong, Z., Li, Y., Li, J., Wang, J., Yang, H., Li, S., Guo, S., Jin, J., Li, R., 2013. Sensor. Actuat. B-Chem. 182(Supplement C), 618-624.

Huang, K., Wang, L., Li, J., Gan, T., Liu, Y., 2013. Measurement 46(1), 378-383.

Hwa, K., Subramani, B., 2014. Biosens. Bioelectron. 62, 127-133.

Jv, Y., Li, B., Cao, R., 2010. Chem. Commun. 46(42), 8017-8019.

Lee, S.J., Yoon, H.S., Xuan, X., Park, J.Y., Paik, S., Allen, M.G., 2016. Sensor. Actuat. B-Chem. 222, 1144-1151.

Lin, X., Ni, Y., Kokot, S., 2016. Biosens. Bioelectron. 79(Supplement C), 685-692.

Lourenço, C.F., Ledo, A., Laranjinha, J., Gerhardt, G.A., Barbosa, R.M., 2016. Sensor. Actuat. B-Chem. 237(Supplement C), 298-307.

Lu, W., Qin, X., Asiri, A.M., Al-Youbi, A.O., Sun, X., 2013. Analyst 138(2), 417-420.

Lu, W., Sun, Y., Dai, H., Ni, P., Jiang, S., Wang, Y., Li, Z., Li, Z., 2016. Sensor. Actuat. B-Chem. 231(Supplement C), 860-866.

Lu, Y., Chen, W., 2012. Chem. Soc. Rev. 41(9), 3594-3623.

Qin, X., Miao, Z., Fang, Y., Zhang, D., Ma, J., Zhang, L., Chen, Q., Shao, X., 2012. Langmuir 28(11), 5218-5226.

Radhakrishnan, S., Kim, H., Kim, B., 2016. Sensor. Actuat. B-Chem. 233, 93-99.

Renard, E., 2002. Curr. Opin. Pharmacol. 2(6), 708-716.

Lee, S., Lee, Y., Park, J., 2013. 2013 IEEE Sens. 1-4.

Schmelzeisen-Redeker, G., Staib, A., Strasser, M., Müller, U., Schoemaker, M., 2013. J. Dia. Sci. Technol. 7(4), 808-814.

Shin, J.H., Marxer, S.M., Schoenfisch, M.H., 2004. Anal. Chem. 76(15), 4543-4549.

Tian, L., Liu, B., 2013. Appl. Surf. Sci. 283, 947-953.

Wang, B., Wu, Y., Chen, Y., Weng, B., Li, C., 2017. Sensor. Actuat. B-Chem.

238(Supplement C), 802-808.

Wang, L., Gao, X., Jin, L., Wu, Q., Chen, Z., Lin, X., 2013. Sensor. Actuat. B-Chem. 176(Supplement C), 9-14.

Wang, N., Burugapalli, K., Song, W., Halls, J., Moussy, F., Ray, A., Zheng, Y., 2013. Biomaterials 34(4), 888-901.

Wang, S., Huang, X., He, Y., Huang, H., Wu, Y., Hou, L., Liu, X., Yang, T., Zou, J., Huang, B., 2012. Carbon 50(6), 2119-2125.

Wang, Z., Cao, X., Liu, D., Hao, S., Du G, Asiri, A.M., Sun, X., 2016. Chem. Commun. 52(100), 14438-14441.

Wang, Z., Cao, X., Liu, D., Hao, S., Kong, R., Du G, Asiri, A.M., Sun, X., 2017. Chemistry 23(21), 4986-4989.

Wilson, G.S., Zhang, Y., Reach, G., Moatti-Sirat, D., Poitout, V., Thevenot, D.R., Lemonnier, F., Klein, J.C., 1992. Clin. Chem. 38(9), 1613-1617.

Wilson, R., Turner, A.P.F., 1992. Biosens. Bioelectron. 7(3), 165-185.

Xie, F., Cao, X., Qu, F., Asiri, A.M., Sun, X., 2018. Sensor. Actuat. B-Chem. 255, 1254-1261.

Xie, F., Liu, T., Xie, L., Sun, X., Luo, Y., 2018. Sensor. Actuat. B-Chem. 255, 2794-2799.

Xie, L., Asiri, A.M., Sun, X., 2017. Sensor. Actuat. B-Chem. 244, 11-16.

Yang, J., Zhang, W., Gunasekaran, S., 2010. Biosens. Bioelectron. 26(1), 279-284.

Yu, B., Moussy, Y., Moussy, F., 2005. Front. Biosci. 10, 512-520.

Yu, Y., Yang, Y., Gu, H., Zhou, T., Shi, G., 2013. Biosens. Bioelectron. 41(Supplement

C), 511-518.

Zhang, D., Fang, Y., Miao, Z., Ma, M., Du, X., Takahashi, S., Anzai, J., Chen, Q., 2013. Electrochim. Acta 107, 656-663.

Zhang, Y., Su, L., Manuzzi, D., de Los Monteros, H.V.E., Jia, W., Huo, D., Hou, C., Lei, Y., 2012. Biosens. Bioelectron. 31(1), 426-432.

Fig.1. The fabrication of needle-type microelectrode. (A) The structure diagram of microelectrode. (B-E) The 3D laser scanning confocal microscope images at different position of microelectrode.

Fig. 2. FESEM images of the Cu nanoflowers with (A) low magnification and (B) high magnification. (C) TEM image of Cu nanoflowers product. (D) EDX spectrum of Cu nanoflowers. (E) X-ray diffraction pattern of Cu nanoflowers. (F) High-resolution X-ray photoelectron spectroscopy survey spectrum of Cu nanoflowers. (G) The principle of operation towards glucose.

Fig. 3. (A) Amperometric responses of biosensors every few days towards various concentration of glucose dropwise added into 0.1 M PBS solution under stirring. (B) Relative sensitivity stability test of the prepared biosensors stored in PBS.

Fig. 4. (A) Amperometric responses of the prepared biosensor towards various concentration of glucose dropwise added into 0.1 M PBS solution under stirring, work potential: 0.6 V vs. Ag/AgCl. (B) Calibration curve of the amperometric responses vs.various glucose concentrations.

Fig. 5. Interference test of prepared biosensor in 0.1 M PBS solution at the working

potential of 0.6 V with 4 mM glucose (twice) and other interfering substance (0.1 mM AA, 0.5 mM UA and 0.1 mM DA).

Fig. 6. In vivo continuous monitoring of glucose concentration in rat. (A) Image of glucose biosensor implantation into rat back. (B) Implanted sensor current response to twice glucose injection. (C) The in vivo response of the implanted sensor to glucose injection (black line) compared with blood glucose values measured from the tail tip tested by a glucose meter (blue line).

Table 1 The comparison of different electrochemical sensors for the determination of glucose.

Electrode	Linear ragne (mM)	Reference
Cu_3P NW/copper foam	0.005-1	(Xie et al., 2017)
Ni_3N NS/Ti mesh	0.0002-1.5	(Xie et al., 2018)
Cu_3N NA/copper foam	0.001-2	(Wang et al., 2017)
NiCoP/Ti mesh	1-10	(Wang et al., 2016)
Porous Ni foam	0.05-7.35	(Lu et al., 2013)
Co_3N NW/TM	0.0001-2.5	(Xie et al., 2018)
Pt/Pani/PVDF/nafion	0-20	(Chen et al., 2015)
GCE/GR-CNT-ZnO/GOD	0.01-6.5	(Hwa and Subramani, 2014)
GCE/Au-ZnO/GOD	1-20	(Fang et al., 2016)
Cu NFs-RGO	0.002-2/2-13	(Wang et al., 2017)
Cu NCs-MWCNTs	Up to 7.5	(Yang et al., 2010)
GCE/Au-RGO/GOD	1-8	(Amouzadeh Tabrizi and Varkani,

		2014)
Micro-Pt/Cu NFs/nafion/GOD/PU	0-20	This work

Highlights

1. A minimally invasive glucose microbiosensor based the flexibly integrated electrode for continuous monitoring glucose in vivo has been developed in this study. This was achieved by coating needle-type microelectrode with Cu nanoflowers, nafion, glucose oxidase (GOD) and polyurethane (PU) membranes, successfully prepared with layer-by-layer deposition.
2. The results supported the suitability of this microsensor for measuring rapid changes of glucose in vivo. This work offers a promising approach in implantable device applications related to diabetes management as well as other medical diagnosis.

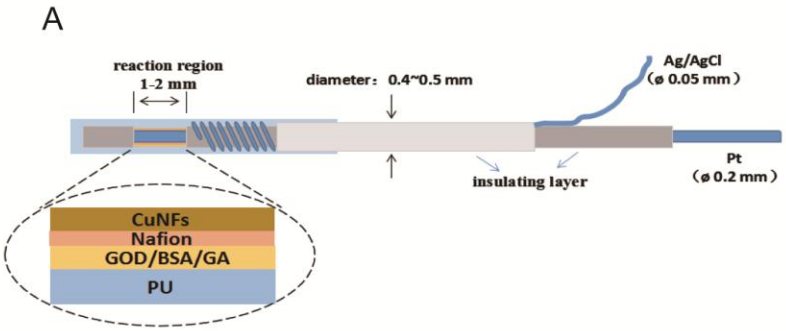
A
reaction region
1-2 mm
diameter: 0.4~0.5 mm
Ag/AgCl
(ø 0.05 mm)
Pt
(ø 0.2 mm)
insulating layer
CuNFs
Nafion
GOD/BSA/GA
PU

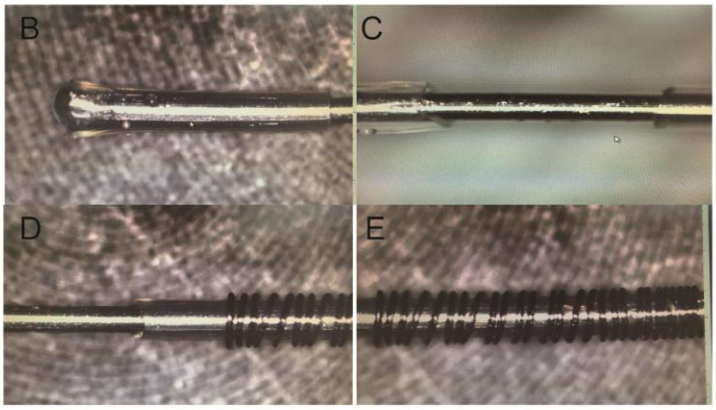
B
C
D
E

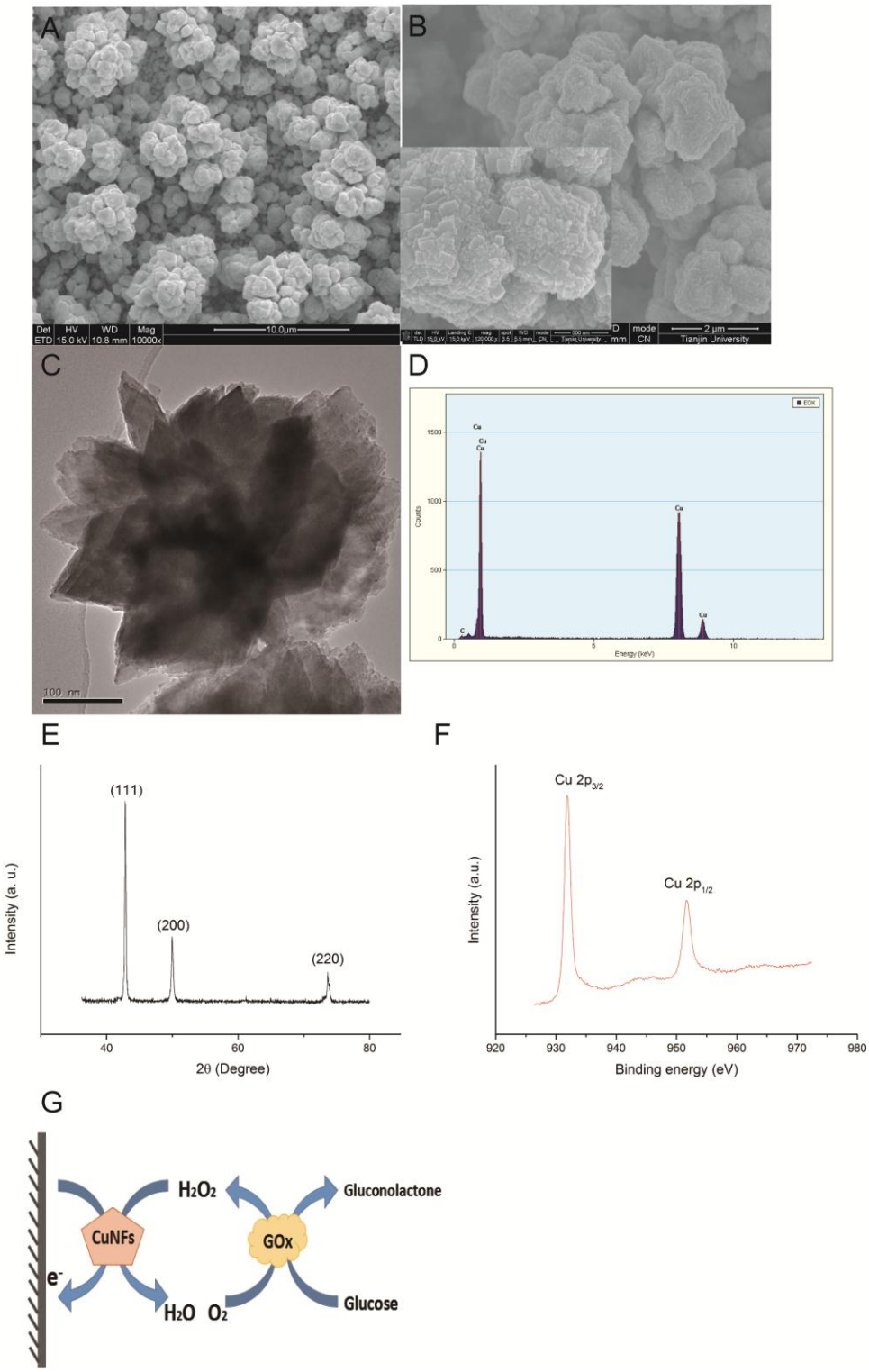
A
B
C
D
E
F
G
(111)
(200)
(220)
Intensity (a. u.)
2θ (Degree)
Cu 2p3/2
Cu 2p1/2
Intensity (a.u.)
Binding energy (eV)
CuNFs
GOx
H2O2
Gluconolactone
Glucose
H2O
O2
e-

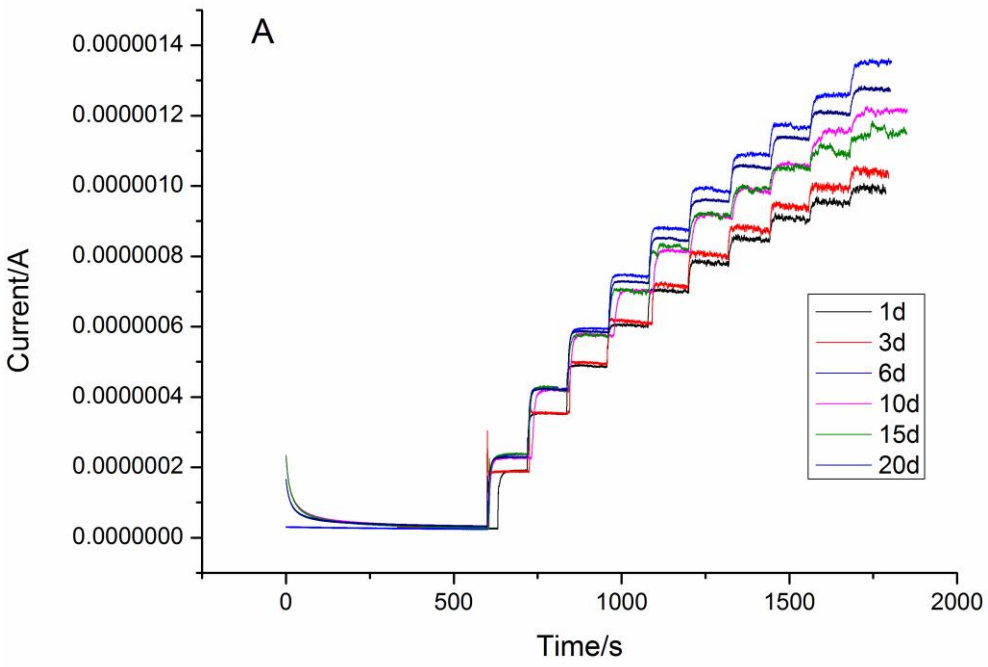
A
Current/A
0.0000014
0.0000012
0.0000010
0.0000008
0.0000006
0.0000004
0.0000002
0.0000000
0
500
1000
1500
2000
Time/s
1d
3d
6d
10d
15d
20d

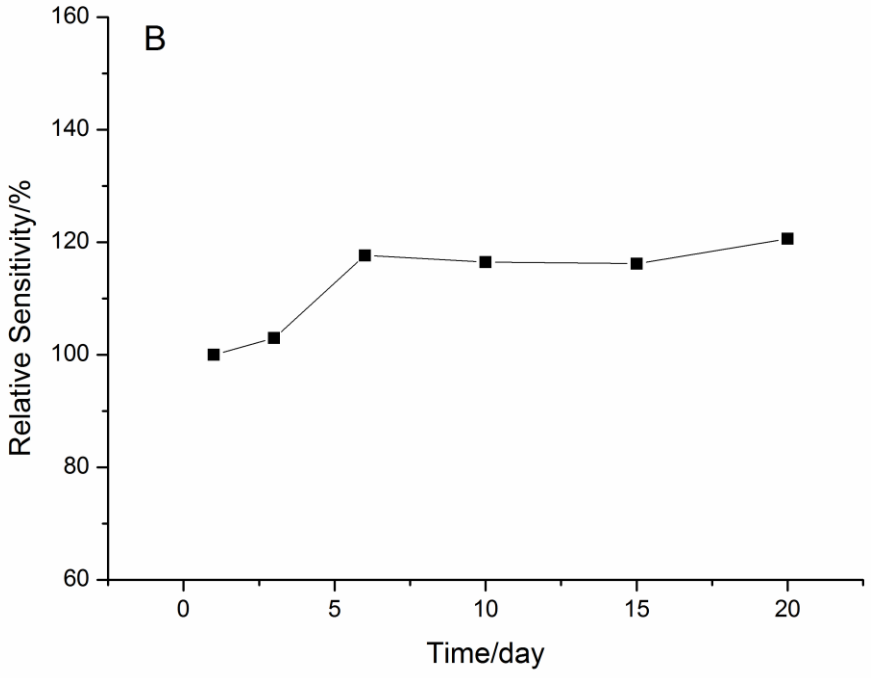
B
Relative Sensitivity/%
160
140
120
100
80
60
0
5
10
15
20
Time/day

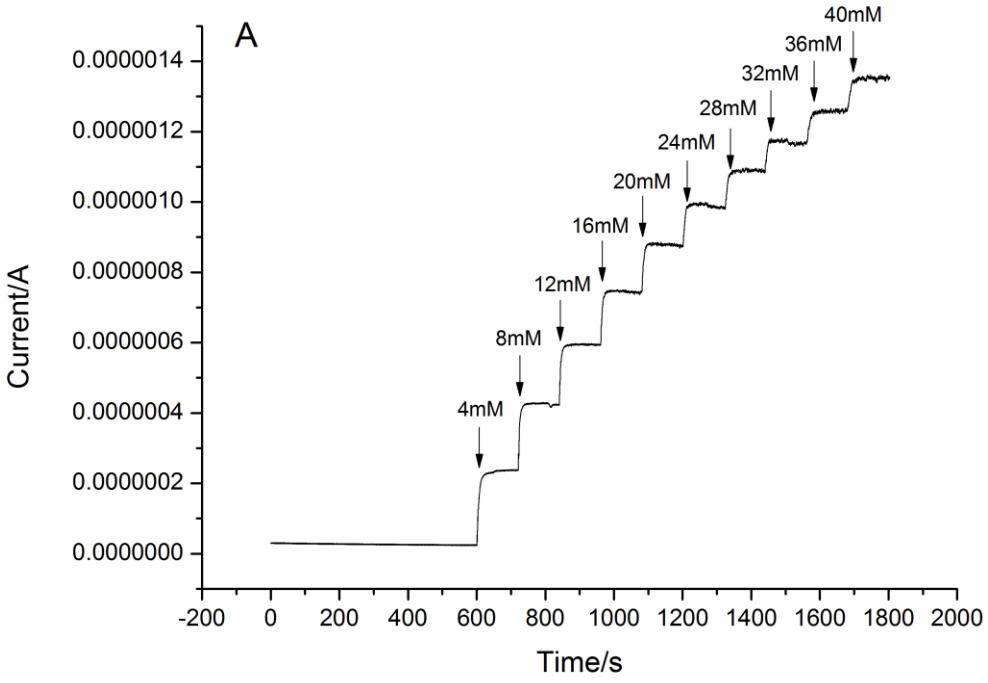
A
Current/A
Time/s
4mM
8mM
12mM
16mM
20mM
24mM
28mM
32mM
36mM
40mM
0.0000014
0.0000012
0.0000010
0.0000008
0.0000006
0.0000004
0.0000002
0.0000000
-200
0
200
400
600
800
1000
1200
1400
1600
1800
2000

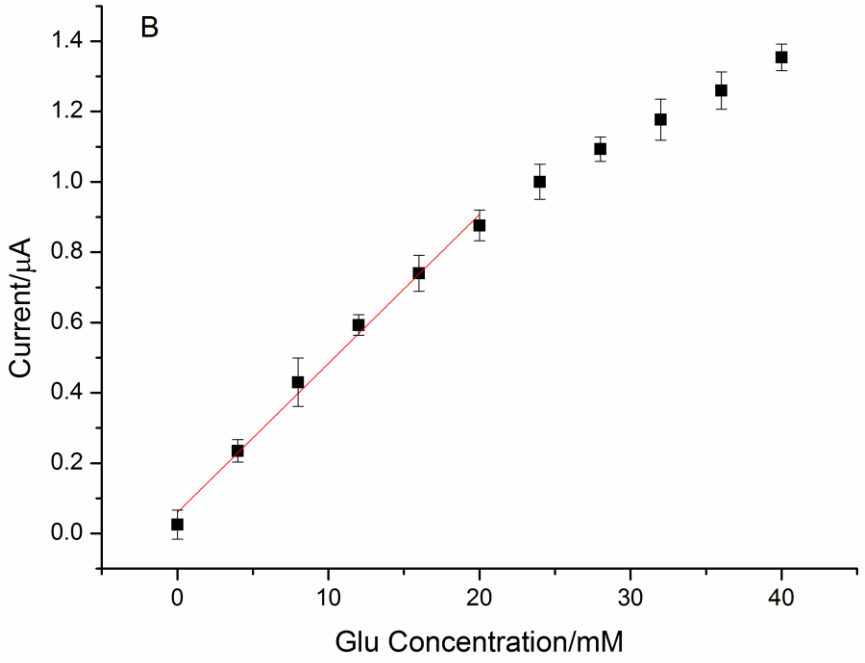
B
Current/μA
Glu Concentration/mM
1.4
1.2
1.0
0.8
0.6
0.4
0.2
0.0
0
10
20
30
40

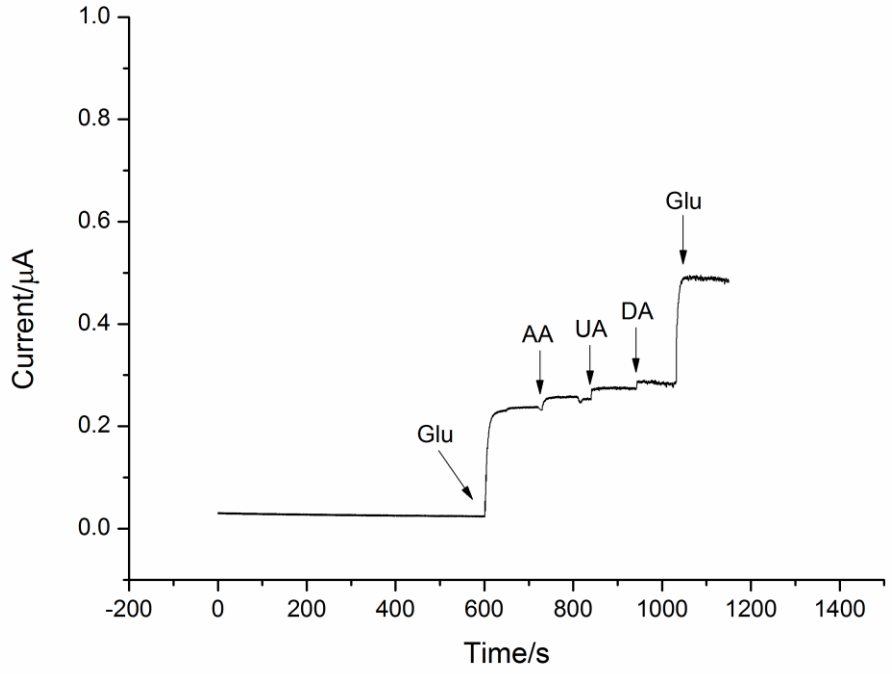

A

B

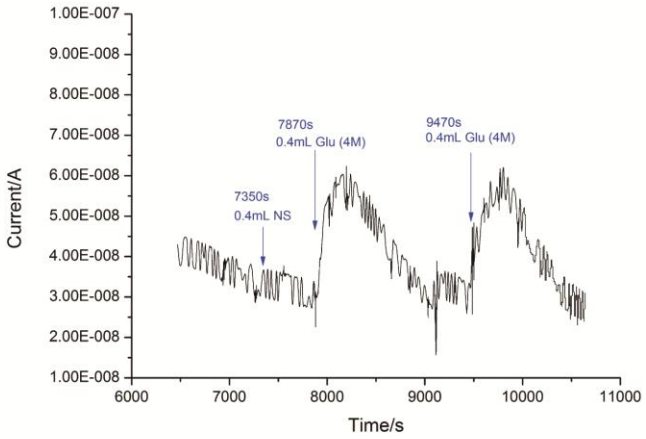

C